



**HAL**  
open science

## **Influence of niobium and titanium introduction on optical and physical properties of silicate glasses**

Nicolas Nowak, Thierry Cardinal, Frédéric Adamietz, Marc Dussauze, Vincent Rodriguez, Laurence Durivault-Reymond, Christine Deneuvilliers, Jean-Eric Poirier

### ► To cite this version:

Nicolas Nowak, Thierry Cardinal, Frédéric Adamietz, Marc Dussauze, Vincent Rodriguez, et al.. Influence of niobium and titanium introduction on optical and physical properties of silicate glasses. Materials Research Bulletin, 2013, 48 (4), pp.1376-1380. 10.1016/j.materresbull.2012.12.004 . hal-00812468

**HAL Id: hal-00812468**

**<https://hal.science/hal-00812468>**

Submitted on 30 Aug 2023

**HAL** is a multi-disciplinary open access archive for the deposit and dissemination of scientific research documents, whether they are published or not. The documents may come from teaching and research institutions in France or abroad, or from public or private research centers.

L'archive ouverte pluridisciplinaire **HAL**, est destinée au dépôt et à la diffusion de documents scientifiques de niveau recherche, publiés ou non, émanant des établissements d'enseignement et de recherche français ou étrangers, des laboratoires publics ou privés.

# Influence of niobium and titanium introduction on optical and physical properties of silicate glasses

Nicolas Nowak<sup>a</sup>, Thierry Cardinal<sup>a,\*</sup>, Frédéric Adamietz<sup>b</sup>, Marc Dussauze<sup>b</sup>, Vincent Rodriguez<sup>b</sup>, Laurence Durivault-Reymond<sup>c</sup>, Christine Deneuvilliers<sup>c</sup>, Jean-Eric Poirier<sup>c</sup>

<sup>a</sup> CNRS – UPR 9048, Université de Bordeaux, ICMCB, 87 av. Dr. A. Schweitzer, Pessac F-33608, France

<sup>b</sup> ISM, UMR 5803 CNRS, Université Bordeaux, 351 Cours de la Libération, Talence F-33405, France

<sup>c</sup> CST COLAS, 4 rue Jean Mermoz, Magny les Hameaux F-78772, France

## ABSTRACT

The effects on optical and mechanical properties of introducing large amounts of TiO<sub>2</sub> and Nb<sub>2</sub>O<sub>5</sub> in a silicate matrix have been studied. Raman spectroscopy has been carried out in order to tentatively establish correlations between structural and physical properties. The high linear refractive index and the increase of the hardness for increasing d<sup>0</sup> ions concentration have been related to the formation of a denser glass network dominated by corner linked NbO<sub>6</sub> and TiO<sub>6</sub> octahedra.

## 1. Introduction

Glasses exhibiting high refractive indices are of importance for the development of new materials and optical systems. They can be used in various applications like optical devices for non-linear optics [1–4], as matrices for fluorescence [5,6], in infrared transmitting devices [7–9], glass ceramics [10–12], thin films for microelectronics [13]. But a high proportion of these glasses incorporate toxic or possible pollutant oxides like PbO, As<sub>2</sub>O<sub>3</sub>, Sb<sub>2</sub>O<sub>3</sub>, or TeO<sub>2</sub>, which provide the high refractive indexes and help to ease the glass processing by lowering the melting temperature. Nowadays for such purpose, friendly glass composition is desirable in order to complain with environmental issues, this subject have sparked off a big industrial interest [14–17]. Bismuth oxide has widely been proposed to replace lead in high refractive index glasses [18–21], but too few data on its toxicity and environment interactions are available which directs us to preferably use metal transition oxides like Ta<sub>2</sub>O<sub>3</sub>, ZrO<sub>2</sub>, La<sub>2</sub>O<sub>3</sub>, TiO<sub>2</sub> or Nb<sub>2</sub>O<sub>5</sub>. Glass containing large amount of metal transition ions have been reported to be attractive. Multiple researches have been devoted on linear and nonlinear optical properties of such material for applications in optical devices [22–24]. Most of the studies report the incorporation of one type of d<sup>0</sup> ions and the evolution of the

optical properties versus the concentration of the transition metal oxide.

In the present article, the incorporation of two metal oxides (TiO<sub>2</sub> and Nb<sub>2</sub>O<sub>5</sub>) has been investigated in sodium and barium silicate matrix. The study shows that the increase of their concentration impacts significantly the optical properties and the glass hardness. Raman and infrared spectroscopies have been carried out to investigate the structure of the glass and to correlate it with the physical characterization.

## 2. Material and methods

### 2.1. Glasses preparation

Two sets of compositions (1) and (2) given below were prepared, varying respectively the niobium oxide content or the titanium oxide content. Reagent grade Na<sub>2</sub>CO<sub>3</sub> (Roth, 99.8%), Ba<sub>2</sub>CO<sub>3</sub> (Alfa Aesar, 99.8%), SiO<sub>2</sub> (Alfa Aesar, 99.8%), TiO<sub>2</sub> (Aldrich, 99.9%) and Nb<sub>2</sub>O<sub>5</sub> (Alfa Aesar, 99.9985%) were mixed, hand milled and melted in a platinum crucible for 30 min at a temperature of 1300–1400 °C depending on the glass composition. The melts were then quenched on a brass plate and immediately annealed at 40 °C below the transition temperature. The glasses obtained are cut and optically polished to obtain final samples of about 1 cm × 1 cm × 1 mm for optical and physical measurements. In the following,  $x_1$  is the NbO<sub>5/2</sub> molar percentage for the first glass system (1) and  $x_2$  is the molar percentage of TiO<sub>2</sub> for the second glass system (2).

\* Corresponding author. Tel.: +33 05 4000 25 43; fax: +33 05 4000 27 61.  
E-mail address: cardinal@icmcb-bordeaux.cnrs.fr (T. Cardinal).

**Table 1**

Glass composition, optical and physical characteristics obtained from glasses of composition (1) and (2): crystallization onset temperature and glass temperature difference  $T_x - T_g$ , linear index  $n_{532}$  measured at 532 nm, volumetric weight  $\varphi$  and microhardness HK.

Sample name	NbO <sub>5/2</sub> (mol.%) ± 0.5	TiO <sub>2</sub> (mol.%) ± 0.5	T <sub>x</sub> - T <sub>g</sub> (°C) ± 3	n <sub>532</sub> ± 0.01	φ (g cm <sup>-3</sup> ) ± 0.005	HK (kg mm <sup>-2</sup> ) ± 5%
x <sub>1</sub>						
N19	18.5	20.1	133	1.89	3.910	602
N23	23	19.0	127	1.90	3.975	606
N26	26.1	18.3	127	1.93	4.037	628
N30	30.3	17.2	123	1.96	4.064	640
N35	34.7	16.2	102	2.00	4.128	664
x <sub>2</sub>						
T20	15.9	20	126	1.87	3.872	591
T25	14.9	25	112	1.91	3.865	610
T30	13.9	30	115	1.95	3.863	631
T35	12.9	35	94	1.99	3.856	640
T40	11.9	40	50	2.00	N/A	(608)

$$(1 - x_1) [24.7\% \text{TiO}_2 - 15.2\% \text{BaO} - 30.5\% \text{SiO}_2 - 29.6\% \text{NaO}_{1/2}] - x_1 [\text{NbO}_{5/2}] \quad (1)$$

$$(1 - x_2) [19.8\% \text{NbO}_{5/2} - 16.1\% \text{BaO} - 30.6\% \text{SiO}_2 - 33.5\% \text{NaO}_{1/2}] - x_2 [\text{TiO}_2] \quad (2)$$

## 2.2. Measurements

For differential scanning calorimetry (DSC), a Netzsch DTA 4040 PC thermoanalyser in air atmosphere was employed with a crushed sample mass of 50–100 mg. Transition temperature (T<sub>g</sub>) at the onset and crystallization temperature (T<sub>x</sub>) were determined using a 15 °C/min heating rate.

Refractive indexes were determined by the Brewster angle technique [25] with a 532 nm laser on one polished side samples for avoiding perturbation from the second side.

Volumetric weight was measured using the Archimedes principle by calculating the difference of a sample mass measured in air and then immersed in calibrated diethyl phthalate (DEP). The accuracy was less than 0.3%. The Knoop microhardness (HK) measurement was performed on a Leica WMHT Auto apparatus equipped with a CCD video camera. A charge of 100 g force (=0.981 N) was applied during 10 s. The average of 10 measurements spread all over the sample was considered to obtain the microhardness of the sample.

Transmission spectra were recorded from 800 nm to 200 nm on a Varian Cary 5000 UV-Visible spectrophotometer and were normalized to a 1 mm thickness for all samples.

Raman spectra from 200 cm<sup>-1</sup> to 2000 cm<sup>-1</sup> were recorded at room temperature on a Labram confocal micro-Raman instrument (Horiba/Jobin-Yvon) in the backscattering geometry, using an excitation at 532 nm and a typical resolution of 3 cm<sup>-1</sup>. The spectrophotometer includes a holographic Notch filter for Rayleigh rejection, a microscope equipped with a 100× objective, and a CCD open electrode nitrogen cooled detector.

Infrared spectra from 100 cm<sup>-1</sup> to 1500 cm<sup>-1</sup> were recorded on reflection mode under dry air atmosphere using a Thermo Scientific Nicolet 6700 spectrometer. Specular reflection spectra were recorded and Kramers–Kronig analyses were performed to obtain the absorption coefficient [25].

## 3. Results

Samples labelling and their corresponding results from thermal measurement T<sub>x</sub> - T<sub>g</sub>, refractive index, measured density and microhardness are gathered in Table 1.

The two specific glasses with x<sub>1</sub> = 34.7% NbO<sub>5/2</sub> (N35) and x<sub>2</sub> = 40% TiO<sub>2</sub> (T40) had to be quenched in a different brass mould with more contact area to avoid crystallization. All the samples

obtained were amorphous to X-ray diffraction and optically transparent; they showed a colour from slight yellow to orange-yellow depending on the d<sup>0</sup> ions content.

The temperature difference T<sub>x</sub> - T<sub>g</sub> decreases with the increasing content of either niobium or titanium oxide, meanwhile both the refractive index, the density and the Knoop microhardness increase. The difference T<sub>x</sub> - T<sub>g</sub> decreases faster in the second glass system when the titanium oxide concentration increases.

Glasses densities evolution as a function of the number of d<sup>0</sup> ions (Nb + Ti) per centimetre-cube is presented in Fig. 1. For the glass system (1), we clearly see a strong increase of density with the increase of niobium content. Additionally, we observe for the glass system (2) a very slight decrease of density when the titanium oxide percentage increases.

Fig. 2 shows the results of the Knoop microhardness tests. The errors bars are deduced from the standard deviation induced by the 10 measurements. We can see for each system an increase of the hardness of the glasses as the niobium oxide or titanium oxide content increases. The maximum value of the hardness is obtained for set (1) at largest niobium oxide content.

Transmission spectra of the glasses from sets (1) and (2) focusing onto the absorption edge ranging from 300 nm to 450 nm are reported in Fig. 3. We observe that the UV absorption edge of the glasses shifts to longer wavelength by increasing the niobium or titanium content. No absorption band due to d<sup>1</sup> ions (Ti<sup>3+</sup> or Nb<sup>4+</sup>) in the 400–900 nm range is observed for all samples (not showed). The absorption edge of the glasses is located between 340 nm and 360 nm for all glasses. The yellow colouring shifting to yellow-orange for high values of x<sub>1</sub> and x<sub>2</sub> is explained by the

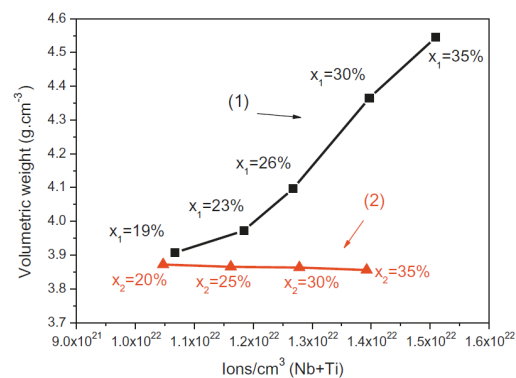


**Fig. 1.** Evolution of volumetric weight as a function of the number of Nb<sup>5+</sup> + Ti<sup>4+</sup> ions per cm<sup>3</sup>.

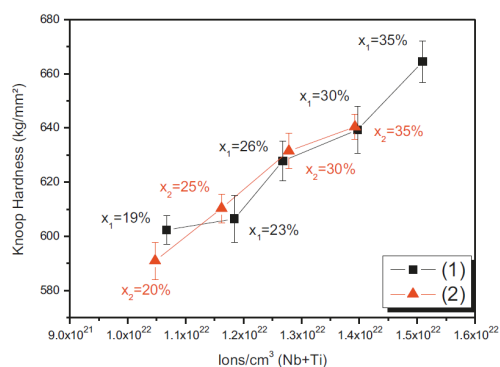


Fig. 2. Evolution of Knoop microhardness as a function of the number of  $\text{Nb}^{5+} + \text{Ti}^{4+}$  ions per  $\text{cm}^3$ .

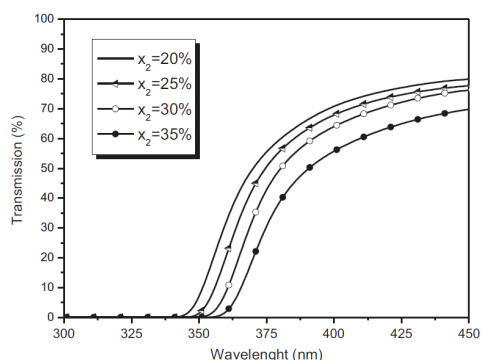
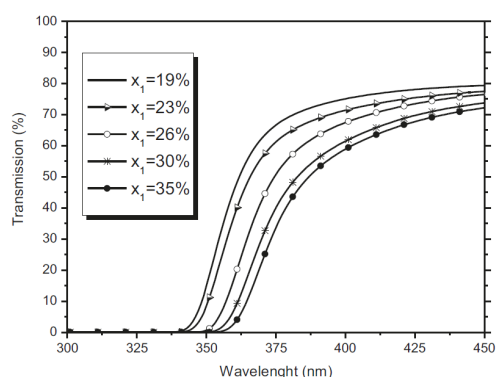


Fig. 3. Absorption spectra of the glasses from (a) set (1) and (b) set (2).

important absorption observed between 350 nm and 450 nm for the sample with high content of  $\text{d}^0$  ions. One can observe in the case of the second glass system that the absorption edge is not as sharp as the one of the first glass system even for the lowest content of  $\text{d}^0$  ions.

Polarized ( $I_{//}$ ) Raman spectra for the two systems are shown in Fig. 4. For both, two main bands are evidenced at  $650 \text{ cm}^{-1}$  and around  $785 \text{ cm}^{-1}$ . A shoulder can be distinguished around  $840 \text{ cm}^{-1}$  for both compositions. The relative intensity of these bands varies depending on the  $\text{d}^0$  ions content. In both glass

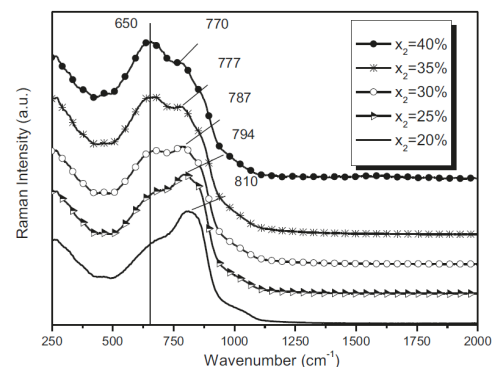
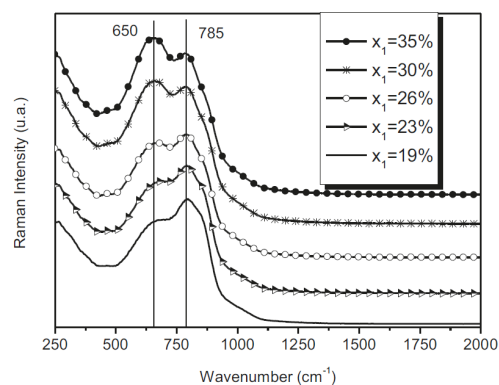


Fig. 4. Polarized Raman spectra  $I_{//}$  of the glasses from (a) set (1) and (b) set (2).

systems the band around  $650 \text{ cm}^{-1}$  becomes more intense in relative intensity as  $x_1$  or  $x_2$  increases. For the band located around  $785 \text{ cm}^{-1}$ , a shift towards lower wavenumber (from  $810 \text{ cm}^{-1}$  to  $770 \text{ cm}^{-1}$ ) is observed when the titanium oxide content increases in the case of set (2) (Fig. 4b). Weaker additional bands can be seen for both compositions between  $850 \text{ cm}^{-1}$  and  $1100 \text{ cm}^{-1}$ .

The IR spectra of glasses are presented Fig. 5. (The curve of the sample with  $x_1 = 12\%$  was not plotted because the data could not be collected for this sample.) For the two compositions we observe similar patterns as well as similar evolution. As the niobium or titanium oxide content increases, the bands observed at  $450 \text{ cm}^{-1}$  and  $580 \text{ cm}^{-1}$  present an increase of their intensity while the one at  $910\text{--}920 \text{ cm}^{-1}$  decreases. The band at  $450 \text{ cm}^{-1}$  shows a greater increase in the case of the second glass system. One band at  $350 \text{ cm}^{-1}$  clearly merge on the spectra from set (1). The band is present in the general shape of the spectra from set (2).

#### 4. Discussion

From the data reported in Table 1, one can conclude that the progressive introduction of  $\text{Nb}_2\text{O}_5$  or  $\text{TiO}_2$  in the glass decreases the "vitreous stability", as the  $T_x - T_g$  parameter decreases, as observed by Malakho et al. [26]. This confirms the strong trend of glasses with high content of transitions ions, especially glasses N35 and T40, to crystallize during the quenching. This effect is confirmed by the fact that the glasses exhibiting the highest  $\text{d}^0$  ions content for the two systems had to be quenched more rapidly. The increase of the refractive index and the density with the



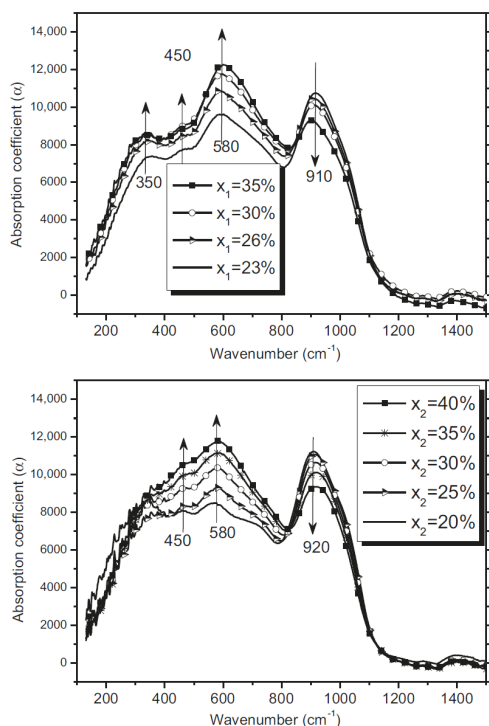


Fig. 5. Infrared spectra of the glasses from (a) set (1) and (b) set (2).

niobium oxide or titanium oxide content is directly correlated to the strong polarisability and high refractive index of the oxides introduced ( $n_{\text{Nb}_2\text{O}_5} = 2.33$ ;  $n_{\text{TiO}_2} \sim 2.50$ ) and their high molar mass compared to the other oxides constituting the glass. Similar high linear refractive index of 2.00 can be achieved for both glass systems even though the polarisability of Ti–O bond is considered higher than Nb–O bond, due to the fact that larger amount of  $d^0$  ions can be introduced in the first glass system.

The increase of the density of the glass with the niobium oxide content for serie (1) is directly related to the fact that the niobium is the heavier ion, and the more niobium is introduced in the glass, the more the network becomes compact and dense. For the second glass system when the titanium content increases, the situation is more complex since the content of the heavier ions decreases, leading to a slight decrease of the volumetric weight. In both systems the microhardness increases, as a function of the number of volume  $d^0$  ions content incorporated in the glass. The evolution seems to be the same for both glasses and only the volume concentration of  $d^0$  ions seems to be the influent parameter. As the total  $d^0$  ions volume concentration is the key parameter, the first glass system is more appropriate when large hardness is desired.

In the transmission spectra of Fig. 3, the bathochromic evolution of the absorption edge can be explained by the fact that the progressive introduction of the transition ions induces new electronic transitions between the 2p orbitals of oxygen atoms and 3d (Ti) or 4d (Nb) orbitals which occurs at lower energies than the ones of the glass matrix, i.e. this introduces a shift of the absorption edge towards larger wavelength. Hence, the colour of the glass slightly changing from pale yellow to yellow-orange has to be related with the long tail of the absorption up to the visible range.

Raman spectroscopy has been widely used for studying the structure of glasses containing  $\text{Ti}^{4+}$  and  $\text{Nb}^{5+}$  ions in oxide matrix. The contributions from  $\text{TiO}_n$  or  $\text{NbO}_n$  polyhedra are dominant in the spectra due to the larger polarisability of these units as compared to silicate, phosphate, borate or germanate units [27]. For niobium oxide containing glasses, the  $650\text{ cm}^{-1}$  band has usually been attributed to the vibration of Nb–O bonds in corner-shared octahedrons associated in 3D blocks [24,26–29]. Zhilin et al. attributed the band to “crystal motif” formed of tungsten bronze like block of  $\text{NbO}_6$  [30]. For the same glasses, a second band around  $840\text{ cm}^{-1}$  is assigned to the vibration of Nb–O bonds in corner-shared in one dimensional chains. A band around  $900\text{ cm}^{-1}$  is attributed to isolated  $\text{NbO}_6$  octahedra with a short Nb–O distance. Raman signal between  $800\text{ cm}^{-1}$  and  $1100\text{ cm}^{-1}$  has been also attributed to Si–O vibration of the  $\text{SiO}_4$  tetrahedra [29].

Regarding titanium containing glasses, bands situated between  $780\text{ cm}^{-1}$  and  $850\text{ cm}^{-1}$  have been attributed to the presence of  $\text{TiO}_n$  polyhedra. In crystalline structure with short Ti–O bond high frequency vibration have been associated to the presence of pyramidal  $\text{TiO}_5$  site, like in  $\text{Ba}_2\text{TiSi}_2\text{O}_8$  ( $825\text{ cm}^{-1}$ ) [31] or  $\text{K}_2\text{Ti}_2\text{O}_5$  ( $905\text{ cm}^{-1}$ ) [32]. The vibration at  $745\text{ cm}^{-1}$  has been related to the vibration of chain of distorted octahedral site like in  $\text{NaTiO}(\text{PO}_4)$  crystalline compound [33]. In titanate compounds, a band at  $650\text{ cm}^{-1}$  can be observed in crystalline  $\text{BaTiO}_3$  in which corner shared connected  $\text{TiO}_6$  octahedra exhibit low distortion.

Looking at the Raman spectra obtained for the glasses of composition (1) presented in Fig. 2a and considering the previous investigations, the increase of the relative intensity of the band at around  $650\text{ cm}^{-1}$  indicates that increasing niobium oxide content induced the formation of a 3D network of corner shared  $\text{NbO}_6$  octahedra. But, the relative intensity of this same band also increases in the case of the second glass system. Such evolution indicates that the titanium polyhedral sites could be also involved in this vibrational mode. One hypothesis is that this vibration band corresponds to the association of  $\text{NbO}_6$  and  $\text{TiO}_6$  octahedra in which the octahedral site has a lower distortion. They together contribute to form a dense 3D network in our glasses. The band in the first system which remains located at around  $785\text{ cm}^{-1}$  can be attributed to one dimensional chains of corner shared distorted octahedra. The occurrence of such association progressively decreases as the niobium oxide content increase. It is supposed that these chains gather to form the dense 3D network. The band around  $850\text{ cm}^{-1}$ , in batch 1 can be attributed to  $\text{NbO}_6$  chains with alternative short and long Nb–O bond length.

The band in the second glass system located around  $810\text{ cm}^{-1}$  shifts to lower wavenumbers as the titanium oxide content increases. As mentioned previously, the mode around  $800\text{ cm}^{-1}$  can be related to the formation of isolated square based pyramids. The shift from  $810\text{ cm}^{-1}$  to  $770\text{ cm}^{-1}$  as the titanium concentration increases may be related to mixed association of  $\text{TiO}_6$  and  $\text{NbO}_6$  units forming more Ti–O–Ti bridges for increasing the Ti/Nb ratio.

From the Raman spectra, the increase of the relative intensity of the band at  $650\text{ cm}^{-1}$  compared to the one at  $780\text{ cm}^{-1}$  seems to indicate that the introduction of niobium and titanium oxides in large amount creates a network with multiples association between  $\text{MO}_6$  entities (M = Ti, Nb) leading a three dimensional  $\text{MO}_6$  network. This conclusion can be related with the strong increase of the density with the  $d^0$  ions content shown before for the first system; the glass network seems to be progressively formed of 3D association of corner shared  $\text{MO}_6$  units. The glass structure becomes then more compact. The hardness evolution is also parallel with the progressive formation of a compact glass network formed of  $\text{MO}_6$  units. The formation of this dense network may be related to this linear evolution of the microhardness.

Concerning the infrared spectra of the glasses presented in Fig. 5, the bands at  $910\text{ cm}^{-1}$  and  $450\text{ cm}^{-1}$  may be assigned to the asymmetric stretching and bending modes, respectively, of the Si–O–Si bonds in the  $\text{SiO}_4$  tetrahedra [28,34]. In Fig. 5a, the  $580\text{ cm}^{-1}$  band may be related to the asymmetric mode of the Nb–O–Nb bonds. The increase of this band with increasing niobium oxide contents are indicative of the formation of corner shared  $\text{NbO}_6$  octahedra, where Si–O–Si bonds are progressively substituted by Si–O–Nb and Nb–O–Nb bonds, which confirms the Raman spectroscopy results discussed previously [34,35]. Since the atomic radius and Pauling electronegativity of  $\text{Ti}^{4+}$  and  $\text{Nb}^{5+}$  are very similar (respectively  $0.68\text{ \AA}$  and  $0.70\text{ \AA}$  for the first parameter and 1.54 and 1.60 for the second), we suppose that the increase of the  $580\text{ cm}^{-1}$  band when increasing the titanium oxide content is attributed to the asymmetric vibrations of Ti–O–Ti bonds which progressively replace Si–O–Ti bonds and the former Si–O–Si bonds. Raman spectroscopy is also in accordance with these results. We attributed the band at  $450\text{ cm}^{-1}$  to bending modes of  $\text{SiO}_4$  units, but its increases as the content of  $d^0$  ions gets greater needs further investigation.

## 5. Conclusions

High refractive indices and harnesses have been obtained in silicate matrices by introducing  $\text{Nb}_2\text{O}_5$  and  $\text{TiO}_2$ . It has been shown that larger niobium concentration than titanium is desirable for achieving high refractive index and high hardness. Correlations have been established between high refractive index, the hardness and the formation of compact glass network with connected  $\text{MO}_6$  octahedra ( $M = \text{Ti, Nb}$ ).

## Acknowledgments

We gratefully acknowledge the “GIS Advanced Materials in Aquitaine” and the French Region Aquitaine for financial support.

## References

- [1] H. Nasu, Y. Ibara, K. Kubodera, J. Non-Cryst. Solids 110 (2–3) (1989) 229–234.
- [2] H. Nasu, J. Matsuoka, K. Kamiya, J. Non-Cryst. Solids 178 (3) (1994) 23–30.
- [3] B.V. Raghavaiah, N. Veeraiyah, J. Phys. Chem. Solids 65 (6) (2004) 1153–1164.
- [4] H. Nasu, T. Ito, H. Hase, J. Matsuoka, K. Kamiya, J. Non-Cryst. Solids 204 (1–2) (1996) 78–82.
- [5] H. Lina, B.S. Tanabeb, L. Linc, Y.Y. Houa, K. Liud, D.L. Yanga, T.C. Maa, J.Y. Yua, E.Y.B. Pund, J. Lumin. 124 (2007) 167–172.
- [6] H. Lin, X.Y. Wang, L. Lin, D.L. Yang, T.K. Xu, J.Y. Yu, E.Y.B. Pun, J. Lumin. 116 (1–2) (2006) 139–144.
- [7] T. Kokubo, M. Nishimura, M. Tashiro, J. Non-Cryst. Solids 22 (1) (1976) 125–134.
- [8] K. Kobayashi, J. Non-Cryst. Solids 316 (2–3) (2003) 403–406.
- [9] A. Pan, A. Ghosh, J. Non-Cryst. Solids 271 (2000) 157–161.
- [10] J.J. Ruiz-Valdés, A.V. Gorokhovskiy, J.I. Escalante-García, G. Mendoza-Suárez, J. Eur. Ceram. Soc. 24 (2004) 1505–1508.
- [11] K. Pengpata, D. Hollandb, J. Eur. Ceram. Soc. 24 (2004) 2951–2958.
- [12] W. Liu, Ch.H. Mao, G.X. Dong, J. Du, Ceram. Int. 35 (2009) 1261–1265.
- [13] R.M. Waser, Curr. Opin. Solid State Mater. Sci. 1 (5) (1996) 706–714.
- [14] J.M. Comte (Corning incorporated), Lead-free glasses exhibiting characteristics of crystals, Canadian Patent 2137122 C (1994).
- [15] S. Wolff, Lead-free optical glasses, US Patent 2003/0040424 A1 (2003).
- [16] M. Morishita, M. Onozawa, 2001. Niobium oxide in environmental friendly optical glass. Proceedings of the international Symposium Niobium 2001, Niobium 2001 Ltd, Bridgeville, USA, (2001) pp. 311–322.
- [17] S.M. Ritter, Lead and arsenic free optical glass with high refractive index, US Patent 2007/0249483 A1 (2007).
- [18] P. Dararutana, S. Pongkrapan, N. Sirikulrat, M. Thawormmongkolkij, P. Wathanakul, Spectrochim. Acta A 73 (3) (2009) 440–442.
- [19] I. Dyamant, D. Itzhak, J. Hormadaly, J. Non-Cryst. Solids 351 (2005) 3503–3507.
- [20] S.-B. Shim et al., Thermochim. Acta, 2009, <http://dx.doi.org/10.1016/j.tca.2009.07.005>.
- [21] J. Fu, J. Non-Cryst. Solids 194 (1996) 207–209.
- [22] M. Abdel-Baki, F. El-Diasty, Curr. Opin. Solid State Mater. Sci. 10 (2006) 217–229.
- [23] M. Abdel-Baki, F.A. Abdel Wahab, F. El-Diasty, Mater. Chem. Phys. 96 (2006) 201–210.
- [24] T. Cardinal, Eur. J. Solid State Inorg. Chem. 33 (1996) 597–605.
- [25] V. Rodriguez, C. Sourisseau, J. Opt. Soc. Am. B 19 (2002) 11.
- [26] A. Malakho, M. Dussauze, E. Fargin, B. Lazoryak, V. Rodriguez, F. Adamietz, J. Solid State Chem. 178 (2005) 1888–1897.
- [27] M.E. Lines, Phys. Rev. B. 43 (14) (1991) 11978–11990.
- [28] L.F. Santos, L. Wondraczek, J. Deubener, R.M. Almeida, J. Non-Cryst. Solids 353 (2007) 1875–1881.
- [29] K. Fukumi, S. Sakka, J. Mater. Sci. 23 (1988) 2819–2823.
- [30] A.A. Zhilin, G.T. Petrovskii, V.V. Golubkov, A.A. Lipovskii, D.K. Tagantsev, B.V. Tayarintsev, A.A. Shepilov, J. Non-Cryst. Solids 345–346 (2004) 182–186.
- [31] S.A. Markgraf, S.K. Sharma, A.S. Bhalla, J. Am. Ceram. Soc. 75 (9) (1992) 2630–2632.
- [32] S. Sakka, F. Miyaji, Fukumi, J. Non-Cryst. Solids 112 (1–3) (1989) 64–68.
- [33] C.E. Bamberger, G.M. Begun, O.B. Cavin, J. Solid State Chem. 73 (2) (1988) 317–324.
- [34] A. Aromne, V.N. Sigaev, B. Champagnon, E. Fanelli, V. Califano, L.Z. Usmanova, P. Pernice, J. Non-Cryst. Solids 351 (2005) 3610–3618.
- [35] M. Dussauze, E.I. Kamitsos, E. Fargin, V. Rodriguez, J. Phys. Chem. C 111 (2007) 14560–14566.